




Performance Evaluation of a Linear Fresnel Concentrator Applying Numerical Simulation

B. E. Tarazona-Romero^{1,2}^a, C. L. Sandoval-Rodriguez^{1,3}^b O. Lengerke-Pérez¹^c,
J. S. Becerra-Reyes¹ and A. Velandia-Esparza¹

¹Automation and Control Energy Systems Research Group (GISEAC), Faculty of Natural Sciences and Engineering, Electromechanical engineering, Unidades Tecnológicas de Santander (UTS), Student Street No 9-82, 680005, Bucaramanga, Colombia

²Energy in Building research group (ENEDI), Doctoral Program in Energy Efficiency and Sustainability in Engineering and Architecture, Department of Machines and Thermal Engines, University of the Basque Country (UPV / EHU), Engineer Torres Quevedo Square, 1, 48013, Bilbao, BI, Spain

³Doctoral Program in Electronic and Communications, Department of Communications Engineering, University of the Basque Country, UPV/EHU, 48013 Bilbao, Spain

Keywords: Lineal Fresnel Concentrator, Numerical Simulation, Performance, Renewable Energy.

Abstract: This work performs an optical analysis of an artisanal system of Linear Fresnel concentrates developed by the Research Group in energy, automation and control systems of the Technological Units of Santander. For this, the numerical simulation methodology was applied by means of the Engineering Equation Solver software. The analysis carried out found that the angle of incidence Theta has a direct relationship with the optical performance of the system, affecting it when the angular inclination is not correct. Additionally, the system increases its performance when the speed and flow of the heat transfer fluid decrease. Finally, the evaluation made to the device despite having a percentage difference with the performance of the real device, serves as a reference to predict the behavior of the system and identify the critical operating characteristics that affect it.


1 INTRODUCTION


Solar energy is a renewable energy source and an alternative to reduce the consumption of fossil fuels and combat the environmental crisis that the world is currently experiencing. Generally, global crises have been the drivers of the growth of renewable energy and solar energy (Moghimi et al., 2017). For example, in 1973-1979 there was the oil and energy crisis, which led to the development of scientific work in order to find reliable sources of alternative energy (Ross, 2016). As a result of these scientific works, the first constructions of solar concentration systems (CSP) began (Pitz-Paal, 2014).


Solar concentration technology is currently one of the most interesting options to reduce the consumption of fossil fuels and greenhouse gas

emissions, widely applied centrally for the production of thermal and electrical energy (Lovegrove & Pye, 2021). CSP systems are based on reflecting direct normal radiation (DNI) through a surface or area of reflection at a focal point of small aperture concentration (Lovegrove & Stein, 2021). A heat transfer liquid circulates through the concentration point that reaches high temperatures, which feed processes with demand for thermal energy or conventional thermodynamic cycles to generate electricity (J. J. C. S. Santos et al., 2018). In general, there are four classes of CSP technologies (Pitz-Paal, 2020): central tower (CT) (Vant-Hull, 2021), Parabolic disk (PD) (Schiel & Keck, 2021), parabolic-trough (PTC) (Moya, 2021) and Linear Fresnel (LFC) (Tarazona-Romero et al., 2021).

Eventually, Linear Fresnel-type Solar Concentrators (LFC) are currently a promising

^a <https://orcid.org/0000-0003-3508-3160>

^b <https://orcid.org/0000-0001-8584-0137>

^c <https://orcid.org/0000-0001-9360-7319>

alternative for the future, due to their simplicity in construction and cost reduction, compared to other CSP technologies. However, they lack popularity and are less mature than PTC systems (Schlecht & Meyer, 2021) (López et al., 2021). The LFC systems have been applied centrally with success, but it still requires more technological developments and research, to overcome the problems that it currently presents (de Sá et al., 2021). Los sistemas LFC están compuestos por filas de espejos planos o levemente curvados (Reflector primario) en dirección transversal y montados sobre una estructura metálica de base, cercano al suelo (Platzer et al., 2021). LFC systems are made up of rows of flat or slightly curved mirrors (primary reflector) in a transverse direction and mounted on a base metal structure, close to the ground (Mills, 2012). The working fluid, generally water, is pumped through the absorber tubes and heated by concentrated solar energy until it partially or totally changes its phase, increasing its enthalpy (Bellos, 2019).

On the other hand, the decentralized LFC system offers advantages over other CSP technologies due to its easy construction, easy access to local resources, modularity, simple operation and maintenance, cost reduction and application of thermosyphon systems, to solve the need of pumping systems (Tarazona-Romero et al., 2021) (Souza et al., 2021). However, these advantages incur a considerable decrease in the efficiency of the system. This makes CFL systems attractive for applications in isolated areas with poverty and high intensity in solar radiation (Tarazona-Romero et al., 2020) (Famiglietti & Lecuona, 2021).

As for the efficiency of a LFC depends strongly on the optical performance of the collector and the thermodynamic behavior of the working fluid in the absorber, the latter not only allows predicting the working conditions of the system, but also allows generating control strategies for avoid equipment damage (A. V. Santos et al., 2021) (Said et al., 2019). The analysis of the performance of the systems can be predicted by means of optical and thermal analyzes through the application of software (Rungasamy et al., 2021). The simulation methods for this type of study can be classified in (Bellos et al., 2019): CFD modeling (Rungasamy et al., 2015), Monte Carlo ray Tracing method (de Sá et al., 2021) and numerical simulations, the latter being the most widely applied, due to the fact that they allow to evaluate and predict the behavior of the device by means of the construction of an algorithm (Ajdad et al., 2019).

Consequently, the research group in energy, automation and control systems (GISEAC) of the Unidades Tecnológicas de Santander (UTS), built and experimented with a LFC artisan prototype developed under the concept of Appropriate Technology for

water heating (Tarazona-Romero et al., 2021) (Tarazona-Romero et al., 2020) and its integration with a desalination system by Humidification-dehumidification. The system is currently in the process of improvement and requires analysis of the optical and thermal performance, which allows predicting its operation and eventually identifying improvement options for its implementation. Based on this, this work develops a numerical simulation of the behavior of the prototype developed by GISEAC in order to evaluate its optical and thermal efficiency.

2 METHODS AND MATERIALS

2.1 Fresnel System Characteristics

In order to carry out an appropriate mathematical model of the system, it is necessary to extract data from the planes of the geometry of the system, Table 1 presents a summary of the dimensions of the evaluated LFC prototype. The real LFC system has an efficiency of 7.19%

Table 1. LFC system dimensions.

Component	Dimensions
Number of Reflective Mirrors	10
Reflective Mirror Length	1 m
Reflective Mirror Width	0.1 m
Number of Absorber Tubes	2
Receiver Tube Outside Diameter	0.003175m
Receiver Tube Inner Diameter	0.0004699m
Absorbent Tubes Length	1.2m
Focal distance	0.75m

Source: Table Prepared by the authors and information taken from (Tarazona-Romero et al., 2021)

Additionally, Table 2 presents another important factor for the development of the simulations and these are the thermodynamic properties of the components of the LFC prototype.

Table 2. Propiedades Termodinámicas Componentes Colector Lineal Fresnel.

Coefficients	Value
Copper tube conduction coefficient	0.8
Copper tube emissivity	0.12
Reflectors mirror reflectance	0.712
Aluminum foil reflectance	0,799
Secondary reflector absorption coefficient	0.93

Source: Table Prepared by the authors and information taken from (Tarazona-Romero et al., 2021)

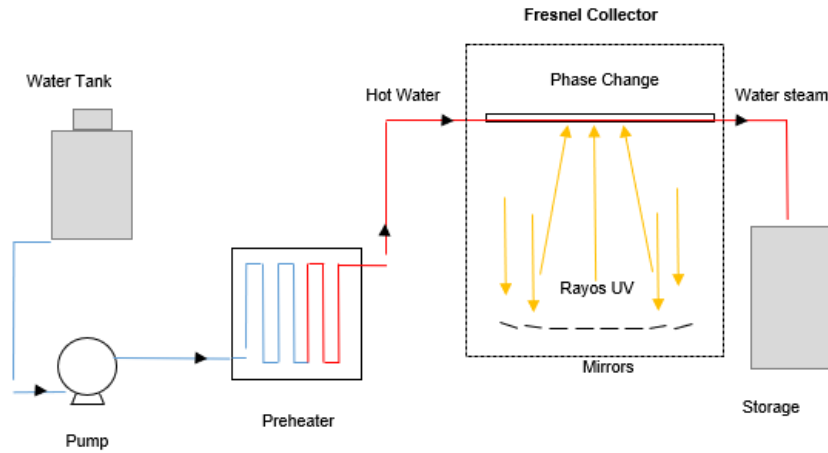


Figure 1: Diagrama prototipo LFC.

Finally, Figure 1 presents the schematization of the evaluated LFC system.

2.2 Simulation Code Considerations

To develop the code corresponding to the behavior of the LFC prototype, the Engineering Equation Solver (EES) software was used and the following considerations were taken into account:

- Dry bulb temperature 25 °C
- Wet Bulb Temperature 22°C
- Humidity 0.72
- Fluid Velocity 0.1 m/s
- Convection heat transfer coefficient 1000 (W/m²·°C)
- Inlet temperature 10 °C
- Outlet temperature 90°
- Theta_T [20, 23, 25, 40, 60]°
- Theta_L [5, 10, 15, 20, 25]°

The simulation process required a series of mathematical models to simulate the behavior of the elements that make up the LFC prototype. The mathematical expression that allows predicting the behavior of the preheater is evidenced in equation 1 (Tarazona-Romero et al., 2021).

$$Q = q_l * L \quad (1)$$

Where, q_l is the heat absorbed by the fluid in (W/m), and L is the length of the fluid's path in (m). The heat absorbed by the fluid can be determined from equation 2.

$$q_l = \pi * (T_p - T_f) * h * diam_{tube} \quad (2)$$

Where, T_p is the temperature of the wall, T_f is the temperature of the fluid, h is the heat transfer

coefficient of film and $diam_{tube}$ represent the diameter of the pipe.

For the analysis of the geometry of the LFC system (Tarazona-Romero et al., 2021), the opening of the collector is taken into account, which is given by the following equation:

$$A_{ac} = W_0 * N * L \quad (3)$$

Where, A_{ac} is the total opening of the collector, W_0 is the width of the mirrors and N refers to the total number of mirrors in the system

Additionally, the width of each reflector must be considered, which is determined from:

$$W_{tot} = W + W_0 \quad (4)$$

$$W = 2 * N * D_w \quad (5)$$

In turn, the focal length of each mirror is given by equation 6:

$$Lfo_i = \sqrt{Lfo^2 + i^2 + D_w^2} \quad (6)$$

Where F is the focal height, on the other hand, i is the mirror counter.

Regarding the angle of position of the absorber (ϕ) it is determined from equation 7:

$$\cos(\phi) = \left[1 + i^2 * \left(\frac{D_w}{Lfo} \right)^2 \right]^{-0.5} \quad (7)$$

On the other hand, the optical efficiency (η_{Optima}) of the system is calculated by applying equation 8:

$$\eta_{optima} = \alpha * \gamma * \rho * \tau * K \quad (8)$$

Where, α is the absorber absorptivity, γ the interception factor, ρ the reflectivity of the mirrors, τ transmittance value and K is the angle of incidence.

The following values are determined within the software:

- α Alpha=0,9
- τ Tau=0,9

- ρ Rho=0,95
- γ Gamma=0,9

The incident angle has two components, one of them is the longitudinal θ_L and the other is the transversal θ_T , then (Ghodbane et al., 2019):

$$K(\theta_L) = \cos(\theta_L) - \frac{Lfo}{L} * \sqrt{1 + \left(\frac{\omega}{4 * Lfo}\right)^2} * \sin(\theta_L) \tag{9}$$

$$K(\theta_T) = \left\{ \cos\left(\frac{\theta_T}{2}\right) - \frac{\frac{w}{4}}{Lfo + \sqrt{Lfo^2 + \left(\frac{w}{4}\right)^2}} * \frac{\sin(\theta_T)}{2} \right\} \tag{10}$$

Additionally, the critical angle (θ_T critic) can be determined by means of the expression (Ghodbane et al., 2019):

$$\theta_{critico} = 94,46 - 2,519 * \left(\frac{W_0}{D_w}\right) - 55,71 * \left(\frac{W_0}{D_w}\right) - 0,48 * \varphi_{medio} + 1,77 * \left(\frac{\varphi_{medio}^2}{1000}\right) + 1,15 * \left(\frac{W_0}{D_w}\right) * \varphi_{medio} \tag{11}$$

And the slope of the mirror is determined through equation 12:

$$\psi = \frac{\phi - \theta_T}{2} \tag{12}$$

Finally, the thermal efficiency of the system is determined by applying the following equation [27]:

$$\eta_{termica} = \frac{Q_{ut}}{Q_{sol}} \tag{13}$$

Where, $\eta_{termica}$ is the thermal efficiency of the system, Q_u the useful heat and Q_s is the available solar irradiation.

3 RESULTS

The simulation process developed in the ESS tool allowed to evaluate the performance of the LFC

Table 4 presents the Results of the ESS for Φ_i , θ_T , K_T , θ_L , K_L , K_a , highlighting:

- θ_T (θ_T) which is defined as the transverse incident angle and K_T which is the component

device. Table 3 presents the values estimated by the data processing code and highlights:

- The heat absorbed (q_l) by the heat transfer fluid at the focal point or solar concentration was 1396 W/m, highlighting that the temperature of the wall of the material through which the fluid circulates was included.
- For its part, the heat density ($Q_{abs,flow}$) through the fluid was 1459 W and the critical theta Angle (θ_{critic}), is presented by the system when it is at an Angle of 72.12°.

Table 3. Results q_l , $Q_{abs,flow}$ and θ_{critic} .

Variable	Results EES
q_l	1396 [W/m]
$Q_{abs,flow}$	1459 [W]
θ_{critic}	72,12 °

Additionally,

of the transverse direction of the total incident angle K_a , shows in the data of

- Table 4 a slight reduction in K_T when Θ_T takes values close to each other, but when Θ_T has values that stray too far or takes higher values, K_T is drastically reduced.
 - For the angle Θ_L (Θ_L) which is defined as the longitudinal incident angle since the projection of the incident angle in the plane is along the length of the collector and K_L is the component of the longitudinal direction of the total incident angle K_a show in the data in Table 4 a slight reduction in K_L with a linear trend.
- Finally, the modifier of the incident angle K_a or also known as (IAM) was determined, which is used to consider the variation of the optical efficiency for the different positions of the sun, it is clear to remember that K_a is made up of the longitudinal and transversal components (K_L y K_T) and that the optical efficiency equation is determined based on it.

Table 4. Results Φ_i , Θ_T , K_T , Θ_L , K_L , K_a .

Item	Φ_i	Θ_T	K_T	Θ_L	K_L	K_a
1	11,31	20	0,9129	5	0,9038	0,825
2	21,8	23	0,8973	10	0,8006	0,7184
3	30,96	25	0,8866	15	0,6914	0,613
4	38,66	40	0,798	20	0,5769	0,4604
5	45	60	0,6589	25	0,4581	0,3018
6	45	60	0,6589	25	0,4581	0,3018
7	38,66	40	0,798	20	0,5769	0,4604
8	30,96	25	0,8866	15	0,6914	0,613
9	21,8	23	0,8973	10	0,8006	0,7184
10	11,31	20	0,9129	5	0,9038	0,825

On the other hand, Table 5 presents the optical efficiency values of the LFC system and highlights:

- The representation of the optical efficiency of the sample presented in Table 5, decreases somewhat because the angles of Θ_T (θ_T) were taken less than the value of Θ_{critic} (θ_{critic}) whose value corresponds to $72,12^\circ$.
- The incidence of the angle Θ_T on the efficiency of the system is maximum as the angle is close to the value of zero (0), however, as Θ_T increases, the efficiency values will decrease, therefore, there is a relationship inversely proportional between angles and optical efficiency

Table 5. Optical Performance of the simulated LFC system.

Θ_T Angle	Optical Performance
20°	57,14%
23°	49,76%
25°	42,46%
40°	31,88%
60°	20,9%
60°	20,9%
40°	31,88%
25°	42,46%
23°	49,76%
20°	57,14%

Finally, the thermal efficiency of the system is determined from the ratio of useful heat and the heat of solar irradiation, the efficiency value presented by the system was 19.32%.

4 CONCLUSIONS

The incidence of the Θ angle is clearly an important factor to take into account when evaluating optical performance, because its variation directly affects other factors inherent to the system's operation. For evaluation of the angle at 20° , an optical performance of 57.14% was obtained and for the evaluation of the system with an angle of 60° , an optical performance of 20.9% was obtained, evidencing the direct relationship between the incidence of the angle and the optical performance of the device.

On the other hand, the speed of the fluid directly influences the overall performance of the device. The current analysis was carried out with a fixed speed of 0.1 m / sec and the thermal efficiency value was 19.32%. The system was evaluated in parallel with a speed of 0.025 m / sec and the performance of the system was 45%, evidencing a direct relationship between performance and flow, that is, the higher the flow, the lower the performance and the lower the flow, the higher the performance. The latter is due to

the fact that the device is designed in a traditional way to handle low flow rates from thermosyphons or small pumping systems.

There is a difference of 12.13% between the efficiency of the real system and the simulation carried out. This is because the simulation method applied to the present analysis could be considered static, as it does not evaluate the system in real time intervals, subjecting the code to solar radiation data that vary with time. However, the development of this type of evaluations allows generating estimates of the behavior in an approximate way.

Finally, the thermodynamic libraries of the ESS software differ a little compared to the thermodynamic tables provided in the bibliography, this may present small changes in calculations made through tools that do not have thermodynamic libraries and require declaring those values manually, for the development of the simulations.

REFERENCES

- Ajdad, H., Filali Baba, Y., Al Mers, A., Merroun, O., Bouatem, A., & Boutammachte, N. (2019). Particle swarm optimization algorithm for optical-geometric optimization of linear fresnel solar concentrators. *Renewable Energy*, *130*, 992-1001. <https://doi.org/10.1016/j.renene.2018.07.001>
- Bellos, E. (2019). Progress in the design and the applications of linear Fresnel reflectors – A critical review. *Thermal Science and Engineering Progress*, *10*, 112-137. <https://doi.org/10.1016/j.tsep.2019.01.014>
- Bellos, E., Tzivanidis, C., & Moghimi, M. A. (2019). Reducing the optical end losses of a linear Fresnel reflector using novel techniques. *Solar Energy*, *186*, 247-256. <https://doi.org/10.1016/j.solener.2019.05.020>
- de Sá, A. B., Pigozzo Filho, V. C., Tadríst, L., & Passos, J. C. (2021). Experimental study of a linear Fresnel concentrator: A new procedure for optical and heat losses characterization. *Energy*, *232*, 121019. <https://doi.org/10.1016/j.energy.2021.121019>
- Famiglietti, A., & Lecuona, A. (2021). Small-scale linear Fresnel collector using air as heat transfer fluid: Experimental characterization. *Renewable Energy*, *176*, 459-474. <https://doi.org/10.1016/j.renene.2021.05.048>
- Ghodbane, M., Boumeddane, B., Said, Z., & Bellos, E. (2019). A numerical simulation of a linear Fresnel solar reflector directed to produce steam for the power plant. *Journal of Cleaner Production*, *231*, 494-508. <https://doi.org/10.1016/j.jclepro.2019.05.201>
- López, J. C., Escobar, A., Cárdenas, D. A., & Restrepo, Á. (2021). Parabolic trough or linear fresnel solar collectors? An exergy comparison of a solar-assisted sugarcane cogeneration power plant. *Renewable Energy*, *165*, 139-150. <https://doi.org/10.1016/j.renene.2020.10.138>
- Lovegrove, K., & Pye, J. (2021). Chapter 2—Fundamental principles of concentrating solar power systems. En K. Lovegrove & W. Stein (Eds.), *Concentrating Solar Power Technology (Second Edition)* (pp. 19-71). Woodhead Publishing. <https://doi.org/10.1016/B978-0-12-819970-1.00013-X>
- Lovegrove, K., & Stein, W. (2021). Chapter 1—Introduction to concentrating solar power technology. En K. Lovegrove & W. Stein (Eds.), *Concentrating Solar Power Technology (Second Edition)* (pp. 3-17). Woodhead Publishing. <https://doi.org/10.1016/B978-0-12-819970-1.00012-8>
- Mills, D. R. (2012). 6—Linear Fresnel reflector (LFR) technology. En K. Lovegrove & W. Stein (Eds.), *Concentrating Solar Power Technology* (pp. 153-196). Woodhead Publishing. <https://doi.org/10.1533/9780857096173.2.153>
- Moghimi, M. A., Craig, K. J., & Meyer, J. P. (2017). Simulation-based optimisation of a linear Fresnel collector mirror field and receiver for optical, thermal and economic performance. *Solar Energy*, *153*, 655-678. <https://doi.org/10.1016/j.solener.2017.06.001>
- Moya, E. Z. (2021). Chapter 7—Parabolic-trough concentrating solar power systems. En K. Lovegrove & W. Stein (Eds.), *Concentrating Solar Power Technology (Second Edition)* (pp. 219-266). Woodhead Publishing. <https://doi.org/10.1016/B978-0-12-819970-1.00009-8>
- Pitz-Paal, R. (2014). Chapter 19—Solar Energy – Concentrating Solar Power. En T. M. Letcher (Ed.), *Future Energy (Second Edition)* (pp. 405-431). Elsevier. <https://doi.org/10.1016/B978-0-08-099424-6.00019-3>
- Pitz-Paal, R. (2020). 19—Concentrating Solar Power. En T. M. Letcher (Ed.), *Future Energy (Third Edition)* (pp. 413-430). Elsevier. <https://doi.org/10.1016/B978-0-08-102886-5.00019-0>
- Platzer, W. J., Mills, D., & Gardner, W. (2021). Chapter 6—Linear Fresnel Collector (LFC) solar thermal technology. En K. Lovegrove & W. Stein (Eds.), *Concentrating Solar Power Technology (Second Edition)* (pp. 165-217). Woodhead Publishing. <https://doi.org/10.1016/B978-0-12-819970-1.00006-2>
- Ross, M. L. (2016). How the 1973 Oil Embargo Saved the Planet. *Foreign Affairs*, *5*.
- Rungasamy, A. E., Craig, K. J., & Meyer, J. P. (2015). 3-D CFD Modeling of a Slanted Receiver in a Compact Linear Fresnel Plant with Etendue-Matched Mirror Field. *Energy Procedia*, *69*, 188-197. <https://doi.org/10.1016/j.egypro.2015.03.022>
- Rungasamy, A. E., Craig, K. J., & Meyer, J. P. (2021). A review of linear Fresnel primary optical design methodologies. *Solar Energy*, *224*, 833-854. <https://doi.org/10.1016/j.solener.2021.06.021>
- Said, Z., Ghodbane, M., Hachicha, A. A., & Boumeddane, B. (2019). Optical performance assessment of a small experimental prototype of linear Fresnel reflector. *Case Studies in Thermal Engineering*, *16*, 100541. <https://doi.org/10.1016/j.csite.2019.100541>

- Santos, A. V., Canavarro, D., Horta, P., & Collares-Pereira, M. (2021). An analytical method for the optical analysis of Linear Fresnel Reflectors with a flat receiver. *Solar Energy*, 227, 203-216. <https://doi.org/10.1016/j.solener.2021.08.085>
- Santos, J. J. C. S., Palacio, J. C. E., Reyes, A. M. M., Carvalho, M., Freire, A. J. R., & Barone, M. A. (2018). Chapter 12—Concentrating Solar Power. En I. Yahyaoui (Ed.), *Advances in Renewable Energies and Power Technologies* (pp. 373-402). Elsevier. <https://doi.org/10.1016/B978-0-12-812959-3.00012-5>
- Schiel, W., & Keck, T. (2021). Chapter 9—Parabolic dish concentrating solar power systems. En K. Lovegrove & W. Stein (Eds.), *Concentrating Solar Power Technology (Second Edition)* (pp. 311-355). Woodhead Publishing. <https://doi.org/10.1016/B978-0-12-819970-1.00007-4>
- Schlecht, M., & Meyer, R. (2021). Chapter 4—Site selection and feasibility analysis for concentrating solar power systems. En K. Lovegrove & W. Stein (Eds.), *Concentrating Solar Power Technology (Second Edition)* (pp. 99-125). Woodhead Publishing. <https://doi.org/10.1016/B978-0-12-819970-1.00015-3>
- Souza, L. F. L. de, Fraidenraich, N., Tiba, C., & Gordon, J. M. (2021). Linear aplanatic Fresnel reflector for practical high-performance solar concentration. *Solar Energy*, 222, 259-268. <https://doi.org/10.1016/j.solener.2021.05.002>
- Tarazona-Romero, B. E., Campos-Celador, A., Muñoz-Maldonado, Y. A., Ascanio-Villabona, J. G., Duran-Sarmiento, M. A., & Rincón-Quintero, A. D. (2021). Development of a Fresnel Artisanal System for the Production of Hot Water or Steam. En M. Botto Tobar, H. Cruz, & A. Díaz Cadena (Eds.), *Recent Advances in Electrical Engineering, Electronics and Energy* (pp. 196-209). Springer International Publishing. https://doi.org/10.1007/978-3-030-72212-8_15
- Tarazona-Romero, B. E., Campos-Celador, A., Muñoz-Maldonado, Y. A., Sandoval-Rodríguez, C. L., & Ascanio-Villabona, J. G. (2020). Prototype of lineal solar collector Fresnel: Artesanal system for the production of hot water and/or water vapor. *Visión Electrónica*, 14(1), Art. 1. <https://doi.org/10.14483/22484728.16013>
- Vant-Hull, L. L. (2021). Chapter 8—Central tower concentrating solar power systems. En K. Lovegrove & W. Stein (Eds.), *Concentrating Solar Power Technology (Second Edition)* (pp. 267-310). Woodhead Publishing. <https://doi.org/10.1016/B978-0-12-819970-1.00019-0>